JOURNAL OF MAGNETIC RESONANCE **126,** 154–157 (1997)
ARTICLE NO. MN971168

COMMUNICATION

Removal of Systematic Errors Associated with Off-Resonance Oscillations in T_2 Measurements

M. Czisch,*,† G. C. King,‡ and A. Ross‡,§

*Bijvoet Center for Biomolecular Research, Utrecht University, Padualaan 8, 3584 CH Utrecht, The Netherlands; and
‡School of Biochemistry and Molecular Genetics, University of New South Wales, Sydney 2052, Australia

Received November 7, 1996; revised March 14, 1997

The CPMG pulse train (*1*) has long been known as a tool for measuring transverse relaxation times in NMR. In the past decade, heteronuclear ^{15}N and ^{13}C T_2 relaxation data have become important in protein NMR, allowing for site-specific characterization of the mobility of the molecule (*2–5*). In a recent publication, we have shown that systematic errors are introduced in T_2 measurements by off resonance effects of the 180° pulses which are used (*6*). These effects produce phase distortions of the signal of interest as well as intensity losses arising from magnetization components aligned along the *z* axis. These unwanted components can lead to a misinterpretation of the relaxation data and therefore to misinterpretation of the protein mobility. In this Communication, we present a method, based on the application of a constant gradient field during the CPMG sequence, which removes these errors.

Figure 1A shows the pulse sequence which can be used to determine the T_2 relaxation rate. In addition to an excitation pulse, it consists of a CPMG block followed by acquisition. If a perfect CPMG block is repeated *n* times in subsequent experiments, the T_2 relaxation can be determined as a function of the signal amplitude: $M_x(n) = M_x(0)\exp(-4\Delta \times n/T_2)$. The CPMG block consists of two ''reduced'' blocks (Δ—180°—Δ), represented by an unitary transformation $\mathbf{U}$. To give proper insight into the development of the magnetization, the time evolution of the density matrix $\boldsymbol{\rho}$ can be calculated according to (*6, 7*)

$$\begin{aligned}\boldsymbol{\rho}_n &= (\mathbf{U}^+)^{2n}\boldsymbol{\rho}_0(\mathbf{U})^{2n}\\ \mathbf{U} &= U_z U_{-y} U_{z'} U_y U_z\\ U_z &\equiv \exp(+i2\pi f_{off}\Delta I_z)\\ U_y &\equiv \exp(+i\Theta(f_1, f_{off})I_y)\\ U_{z'} &\equiv \exp[+i\phi(f_1, f_{off})I_z]\end{aligned} \qquad [1]$$

† To whom correspondence should be addressed.

§ Present address: Hoffmann-La Roche AG, CH-4070 Basel, Switzerland.

with

$$\begin{aligned}\Theta(f_1, f_{off}) &= \arctan\left(\frac{f_1}{f_{off}}\right)\\ \phi(f_1, f_{off}) &= \pi\sqrt{1 + \left(\frac{f_{off}}{f_1}\right)^2}\end{aligned} \qquad [2]$$

and f_1 and f_{off} denote the RF field strength and the offset, respectively. Although correct, this representation somehow hides the off-resonance effects under discussion. As described earlier, it is more convenient to combine the five rotations in the reduced block (Eq. [1]) into a single rotation by an angle ϕ_{eff} around an effective axis (*6, 8*). This effective axis has a tilt angle Θ_{eff} with respect to the frame of reference (Fig. 2) and is located in the *xz* plane if the 180° pulses are applied parallel to the *x* axis. The complete propagator for the reduced block now reads

$$\begin{aligned}\mathbf{U} = &\exp[+i\Theta_{eff}(f_{off}, f_1, \Delta)I_y]\\ &\times \exp[-i\Phi_{eff}(f_{off}, f_1, \Delta)I_z]\\ &\times \exp[-i\Theta_{eff}(f_{off}, f_1, \Delta)I_y].\end{aligned} \qquad [3]$$

Φ_{eff} and Θ_{eff} can be calculated as described previously (*6*) leading to the expression,

$$\begin{aligned}\cos\frac{\phi_{eff}}{2} = &\cos(2\pi f_{off}\Delta)\cdot\cos\left\{\frac{\pi}{2}\left[1 + \left(\frac{f_{off}}{f_1}\right)^2\right]^{1/2}\right\}\\ &- \sin(2\pi f_{off}\Delta)\frac{\sin\left\{\frac{\pi}{2}\left[1 + \left(\frac{f_{off}}{f_1}\right)^2\right]^{1/2}\right\}}{\left[1 + \left(\frac{f_1}{f_{off}}\right)^2\right]^{1/2}}\end{aligned}$$

$$\begin{aligned}\tan(\Theta_{eff}) = &\sin(2\pi f_{off}\Delta)\\ &\times \cot\left\{\frac{\pi}{2}\left[1 + \left(\frac{f_{off}}{f_1}\right)^2\right]^{1/2}\right\}\cdot\left[1 + \left(\frac{f_{off}}{f_1}\right)^2\right]^{1/2}\\ &+ \cos(2\pi f_{off}\Delta)\cdot\frac{f_{off}}{f_1}.\end{aligned} \qquad [4]$$

1090-7807/97 $25.00

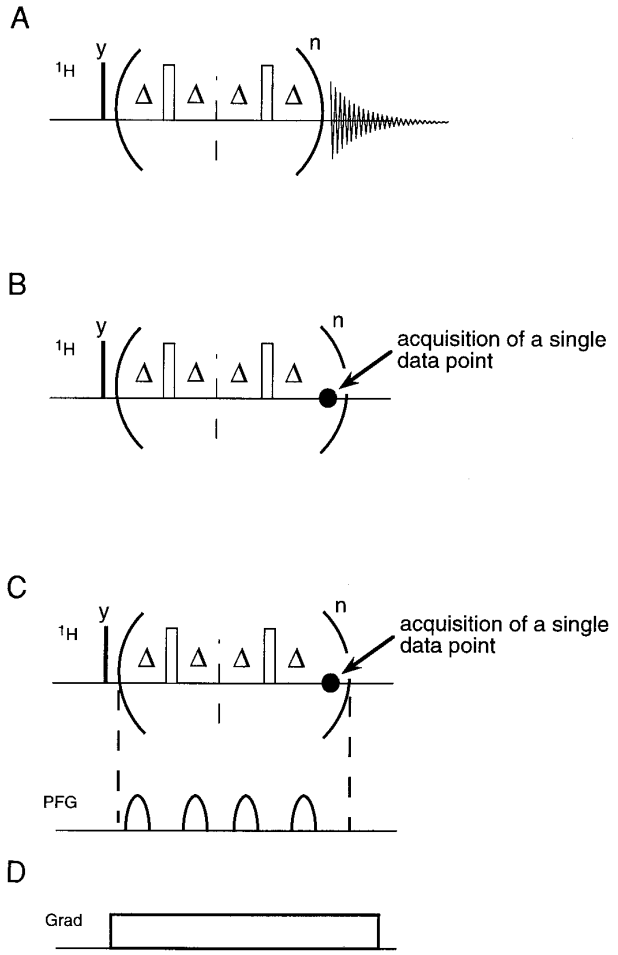

FIG. 1. Pulse sequences used to demonstrate the off-resonance effects of the CPMG sequence. Narrow bars indicate hard 90° excitation pulses, open bars correspond to 180° pulses of length 100 μs. Δ was set to 450 μs, resulting in a total time of the basic CPMG block of 2 ms. (A) Basic sequence used to determine the transverse relaxation time. (B) Pulse sequence to monitor the oscillations due to off-resonance effects. A single data point is measured at the end of each CPMG repetition. A FID of 128 points was acquired by performing $n = 128$ repetitions. (C) Same as (B) but using sine-shaped PFGs of 0.314 G/cm flanking the reduced CPMG block, and (D) using a constant B_0 gradient throughout the complete CPMG sequence. The gradient was applied with 0.2 G/cm. All experiments were performed with a two-step phase cycling (y, $-y$) on the excitation pulse and the receiver.

The major advantage of this representation lies in the fact that multiple repetitions of the CPMG block are just expressed by a multiplication of the effective flip angle:

$$\begin{aligned}\mathbf{U}_{\mathrm{CPMG}} \equiv \mathbf{U}^{2n} = \exp[+i\Theta_{\mathrm{eff}}(f_{\mathrm{off}}, f_1, \Delta)I_y] \\ \times \exp[-i(2n)\Phi_{\mathrm{eff}}(f_{\mathrm{off}}, f_1, \Delta)I_z] \\ \times \exp[-i\Theta_{\mathrm{eff}}(f_{\mathrm{off}}, f_1, \Delta)I_y]. \qquad [5]\end{aligned}$$

Assuming that the starting magnetization is aligned on the x axis, an effective flip angle which deviates from 180° leads to an oscillation of the magnetization around the effective axis, dependent on both the offset frequency and the RF field strength applied. As was shown previously, these oscillations give rise to systematic errors in the T_2 measurements (*6*).

To demonstrate this oscillating component, the pulse sequence of Fig. 1B was performed. The envelop of the transverse decay is monitored here by acquiring a single data point at the end of each repetition of the CPMG block. If 128 repetitions are performed, this therefore leads to a FID of 128 points. A FT decomposes the signal into a nonoscillating component at zero frequency (representing the magnetization of interest in a T_2 measurement) and sidebands with the frequency of the rotation around the effective field.

Figure 3A shows a series of 1D experiments for offset frequencies ranging from 0 to 5850 Hz, incremented in steps of 150 Hz. The experiment was performed on a doped water sample with the length of the 180° pulses adjusted to 100 μs to mimic the situation frequently found for ^{15}N refocusing pulses at high-field spectrometers using triple resonance and/or 8 mm probe heads. In Fig. 1C, PFGs flanking the reduced block are introduced. The corresponding experiment with a sine-shaped gradient of 400 μs length and a strength of 0.314 G/cm is shown in Fig. 3B.

Figure 1D gives the constant-gradient sequence. Keeping all other experimental parameters equal, the gradient is switched on at the beginning of the CPMG sequence and is constant throughout the complete experiment. The result for a gradient strength of 0.2 G/cm is shown in Fig. 3C. This demonstrates clearly that the oscillating component is efficiently suppressed by the application of the gradient. A slight reduction of the intensity of the nonoscillating component was found (Fig. 4). The signal losses arise partly due to

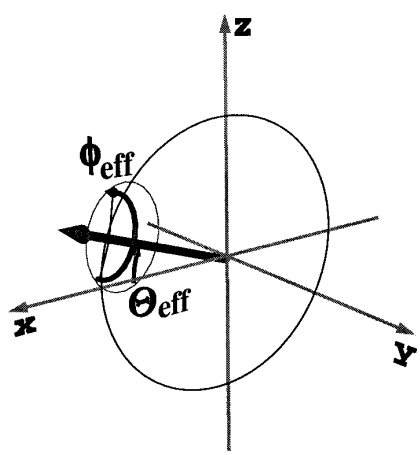

FIG. 2. Pictorial representation of the effective rotation of the reduced block of the CPMG sequence given in Eq. [5]. The angle $\Theta_{\mathrm{eff}}(x, y)$ describes the tilt angle of the effective field indicated by the bold arrow, $\Phi_{\mathrm{eff}}(x, y)$ refers to the angle of precession about this field, using normalized coordinates as defined in Eq. [4]. For emphasis, the figure shows the result for an odd number of repetitions of the reduced block. At reasonable offsets and for even numbers of repetitions, the magnetization ends up close to the x axis.

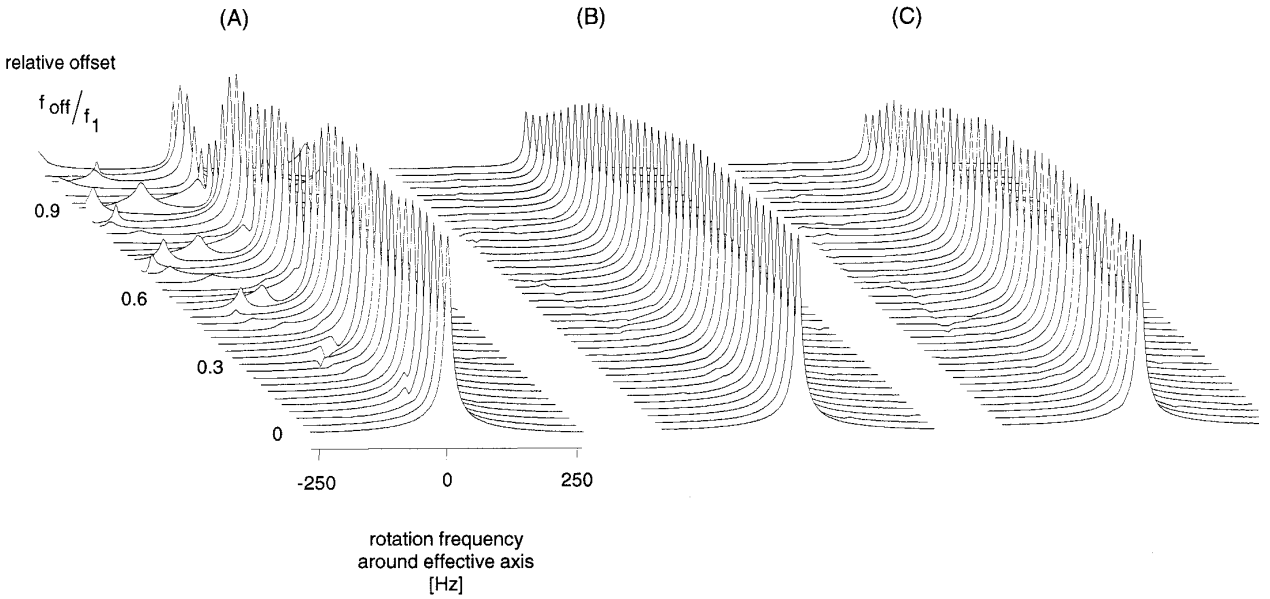

FIG. 3. Result of the experiments described in Figs. 1B–1D with a RF field of 5 kHz ($= f_1$, see Eq. [1]). A doped water sample was used. For each off-resonance frequency f_{off} (Eq. [1]) (ranging from 0 to 5850 Hz in steps of 150 Hz), 128 points were acquired, Fourier transformed, and plotted in magnitude mode. The offset axis is shown in relative units f_{off}/f_1. Besides the nonoscillating component at zero frequency, the 1D spectra in (A) show side bands reflecting magnetization components that introduce systematic errors. In (B) and (C) the identical experiment was performed using PFGs and a constant B_0 gradient during the CPMG sequence as given in Figs. 1C and 1D, with the gradient strength of 0.314 and 0.2 G/cm, respectively. Note the suppression of the side bands.

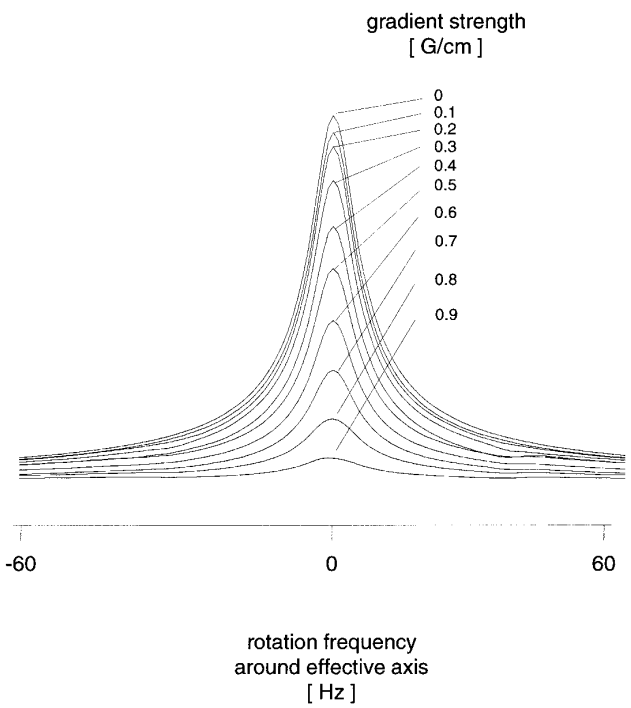

FIG. 4. The reduction of signal intensity of the nonoscillating component due to the constant gradient is shown for several gradient strengths. The graph shows the on-resonance case. Gradient values above 0.5 G/cm are only shown for comparison and are of no practical importance.

diffusion effects (*9*), especially if a stronger B_0 gradient is applied. For a gradient strength below 0.8 G/cm, no broadening of the lines is noticed (Fig. 4). Diffusion effects become less significant if the sequence is run on a sample with high molecular weight. Finally, diffusion effects can be corrected for by running the experiment at several gradient strengths.

Another source of the signal loss is the fact that the magnetization at the first 180° pulse of the CPMG sequence is no longer aligned along the *x* axis but shows all possible phases (if the gradient is sufficiently strong). Therefore, the sequence is no longer a perfect CPMG but a mixture of CPMG and CP (*10*) sequences. Due to the nonperfect refocusing pulses and the B_1 inhomogeneity, the CP part leads to the well-known signal reduction. Changing the phase of the excitation pulse does not change the outcome of the experiment (data not shown). Nevertheless, the signal loss is more than compensated by the removal of the oscillations.

The effect of both the constant gradient and the PFGs can be explained in two ways: (a) The gradient leads to a slightly different precession frequency dependent on the spatial location in the sample. This corresponds to an effective spatially dependent offset (or a spatially dependent phase of the magnetization in the case of PFGs); therefore phase errors are averaged, which corresponds to an integration over f_{off} in Eq. [4]. This also explains the observation that the offset dependency of the intensity of the nonoscillating component is less pronounced using a gradient. (b) In addition to the

fact that a spin echo must be created by the CPMG sequence, now the condition for a gradient recalled echo also must be fulfilled. Magnetization pathways not perfectly refocused at the time of acquisition are efficiently dephased by the gradient and thus no longer contribute to the final signal.

The advantage of the constant-gradient experiment vs the PFG setup lies in the fact that there are just two gradient switching points. Influences of eddy currents are therefore minimized. It is also difficult, if not impossible, on some older spectrometer systems to implement a high number of PFGs. A drawback of the constant gradient is the fact that, for a strong gradient or far off-resonance, the Larmor condition for the RF pulses is no longer matched exactly. This may lead to minor distortions of the nonoscillating component (as visible in Fig. 3C).

In conclusion, we have shown that systematic errors in the measurements of transverse relaxation times caused by oscillations due to weak B_1 field strength can be removed by the application of a constant-gradient field during the CPMG period or by a series of PFGs flanking the reduced CPMG block. To the best of our knowledge, this is the first application of a constant-gradient field during RF pulsing periods in high-resolution NMR.

ACKNOWLEDGMENTS

The spectra shown were recorded at the SON NMR Large-Scale Facility. This work was supported by the European Community TMR program (Contract ERBFMGECT950032) (to M.C.) and by the Australian Research Council (to G.C.K.). We thank G. W. Vuister and R. Boelens for discussion, and M. Tessari and R. Weisemann for help carrying out the experiments on the Varian and Bruker systems, respectively. Pulse sequences for UnityPlus and DMX systems will be provided on request.

REFERENCES

1. S. Meiboom and D. Gill, *Rev. Sci. Instrum.* **29,** 688 (1958).
2. L. E. Kay, D. A. Torchia, and A. Bax, *Biochemistry* **28,** 8972 (1989).
3. N. R. Nirmala and G. Wagner, *J. Am. Chem. Soc.* **110,** 7557 (1988).
4. P. G. Schmidt, H. Sierzputowska-Gracz, and P. F. Angris, *Biochemistry* **26,** 8529 (1987).
5. J. W. Peng and G. Wagner, *Methods Enzymol.* **239,** 563 (1994).
6. A. Ross, M. Czisch, and G. C. King, *J. Magn. Reson.* **124,** 355 (1997).
7. R. R. Ernst, G. Bodenhausen, and A. Wokaun, ''Principles of Nuclear Magnetic Resonance in One and Two Dimensions,'' p. 120, Clarendon Press, Oxford, 1992.
8. J. P. Elliott and P. G. Dawber, ''Symmetry in Physics,'' Vol. 2, p. 480, Macmillan, London, 1979.
9. J. Keeler, R. T. Clowes, A. L. Davis, and E. D. Laue, *Methods Enzymol.* **239,** 145 (1994).
10. H. Y. Carr and E. M. Purcell, *Phys. Rev.* **94,** 630 (1954).